2012

22nd International Lightning Detection Conference
2 – 3 April • Broomfield, Colorado, USA
4th International Lightning Meteorology Conference
4 – 5 April • Broomfield, Colorado, USA

INFLUENCE OF INITIAL CONDITIONS ON LIGHTNING FORECASTING USING THE WRF MODEL

G. S. Zepka, O. Pinto Jr., A. C. V. Saraiva
National Institute for Space Research – INPE, São José dos Campos, SP, Brazil
giselezepka@gmail.com

1. INTRODUCTION

Improved forecasts of the timing and location of thunderstorms and associated lightning are of great interest to all persons concerned with protecting life and property. Particularly during the warm season, it is essential the use of high-resolution forecast tools to provide a detailed description of the mesoscale weather features, which are frequently responsible by the primary forcing convection.

Comparing to the past, the skill of numerical weather prediction has improved enormously, mainly because of substantial increases in computational power and more efficient numerical techniques. Moreover, due to the chaotic behavior of the atmosphere (Lorenz, 1965), considerable efforts are continuously employed for a more comprehensive and accurate representation of the physical processes within the models. However, in terms of the regional models, one complex limitation is the uncertainty with respect the initial and lateral boundary conditions provided by the global models (Warner et al., 1997). The uncertainties associated with the model initialization can decrease the reliability of the deterministic forecasts. Since it is not easy to exactly separate the errors due to the initial conditions from those due to model deficiencies, there has been considerable interest in the investigation of the sensitivity of forecast errors to initial conditions.

The present study examines the impact of initializing the Weather Research and Forecasting (WRF) model (Skamarock et al., 2008) with Global Forecast System (GFS) analyses and forecasts fields of 1 and 0.5-degree grid increment resolutions. Short-range simulations of ten thunderstorm cases were performed with high space WRF model resolution to develop a methodology to qualitatively forecast lightning occurrence with few hours in advance during the summer season in southeastern Brazil. The influence of the same initialization dataset but with different resolutions over the WRF model will be evaluated comparing the lightning forecasting maps for two additional thunderstorm cases, one without lightning occurrence, and calculating statistical scores to help in the forecasting verification.

2. LIGHTNING DATA

Cloud-to-ground (CG) lightning flash data provided by the Brazilian lightning detection network (BrasilDAT) (Pinto Jr. et al., 2007; Pinto Jr., 2009) from October 2008 to March 2009 were used in this study. It is observed that in southeastern Brazil the detection efficiency of CG flashes is approximately 90% (Ballarotti et al., 2006; Saraiva et al., 2011). For this reason, in Figure 1, the red rectangle indicates the region of interest covering the eastern half of São Paulo state, the southern portion of Minas Gerais state and the western portion of Rio de Janeiro state. This area also coincides with the WRF nested domains of higher horizontal resolution ($DOM3_{(0.5-deg)}$ and $DOM4_{(1-deg)}$) to be presented in the next section.

To ensure the homogeneity of the meteorological patterns associated with the lightning occurrence, we adopt as a criterion to select days with a continuous lightning activity of at least four hours, and with more than 400 CG lightning flashes per hour. Ten days were selected and characterized as isolated and/or multicellular non-severe thunderstorms. Table 1 shows the time period, total lightning flashes detected, and meteorological conditions responsible for the lightning occurrence in each case.

3. WEATHER RESEARCH AND FORECASTING (WRF) MODEL

The fully compressible and non-hydrostatic atmospheric WRF model version 3.3.1, coded with a terrain-following hydrostatic-pressure vertical coordinates (Skamarock et al., 2008), was implemented to process the simulations. During the simulation period of 24 hours, the 0000 UT Global Forecast System (GFS) gridded analysis fields and 3h-interval forecasts with 1 and 0.5-degree horizontal grid resolution were

used to initialize the model and nudge the boundaries of the coarse domains. As showed in Figure 1 and Table 2, two model setups were established according to the GFS resolution used as input data. The nested domains DOM3$_{(0.5\text{-deg})}$ and DOM4$_{(1\text{-deg})}$ matched in terms of geographical location and number of grid points. In the vertical direction, 31 unevenly spaced full sigma levels were selected. The physical model parameterizations are presented in Table 3.
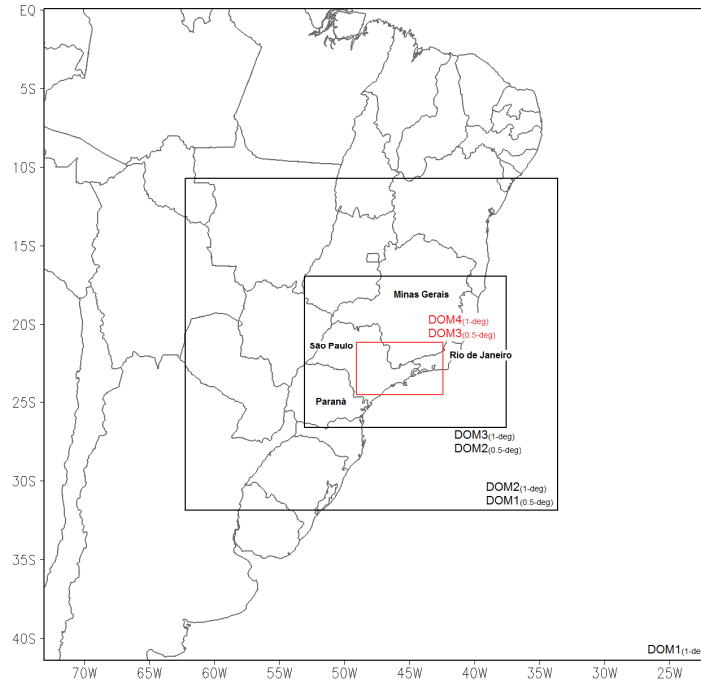

Figure 1 – The WRF domains (see Table 2 for details). The red rectangle encloses the DOM3$_{(0.5\text{-deg})}$ and DOM4$_{(1\text{-deg})}$, and indicates the region of interest from where lightning data were analyzed.

Table 1 – List of thunderstorm days investigated.

Date	Time Period	Total Flashes	Meteorological Condition
11/26/2008	1530-2130 UT	9647	Local Convection / South Atlantic Convergence Zone
12/22/2008	1530-2130 UT	8357	Trough in the middle and upper troposphere / Local Convection
01/30/2009	1530-2330 UT	11437	Trough in the middle and upper troposphere / Subtropical Jet / Extratropical Cyclone
01/31/2009	1730-2230 UT	7985	Trough in the middle and upper troposphere / Subtropical Jet / Extratropical Cyclone
02/07/2009	1530-2330 UT	10671	Local Convection
02/08/2009	1530-2330 UT	13462	Subtropical Jet / Local Convection
02/10/2009	1630-2230 UT	9821	Bolivian High / Local Convection
02/22/2009	1530-2230 UT	14458	Local Convection
02/24/2009	1430-2230 UT	14589	Subtropical Jet / Local Convection
03/07/2009	1430-2330 UT	14533	Local Convection / Frontal System
Total:	**71 hours**	**114960 flashes**	

Table 2 – Configuration of WRF domains according to the resolution of GFS input data. For WRF runs with 1-degree GFS data, the setup was: DOM1 (54 km), DOM2 (18 km), DOM3 (6 km), and DOM4 (2 km). For WRF runs with 0.5-degree GFS data, the setup was: DOM1 (18 km), DOM2 (6 km), and DOM3 (2 km). The region of interest matches with the domains marked in bold.

Model Setup	Horizontal Resolution	Geographic Coordinates
DOM1$_{(1\text{-deg})}$	54 km	41.40^o S to 0.07^o N 73.09^o W to 21.69^o W
DOM2$_{(1\text{-deg})}$ DOM1$_{(0.5\text{-deg})}$	18 km	31.73^o S to 10.78^o S 62.12^o W to 33.73^o W
DOM3$_{(1\text{-deg})}$ DOM2$_{(0.5\text{-deg})}$	6 km	24.53^o S to 21.13^o S 49.07^o W to 42.42^o W
DOM4$_{(1\text{-deg})}$ **DOM3$_{(0.5\text{-deg})}$**	**2 km**	**26.45^o S to 16.81^o S** **52.95^o W to 37.50^o W**

Table 3 – Model physical parameterizations.

Physics Category	Parameterization
Microphysics scheme	Thompson (Thompson et al., 2004)
Cumulus scheme	Grell-Devenyi ensemble (Grell and Devenyi, 2002)
PBL turbulence scheme	Yonsei University (YSU) (Noh et al., 2003)
Surface layer scheme	Similarity Theory
Land-surface model scheme	Noah (Chen and Dudhia, 2001)
Shortwave radiation scheme	Dudhia (Dudhia, 1989)
Longwave radiation scheme	Rapid Radiative Transfer Model (RRTM) (Mlawer et al., 1997)

4. FORECASTING METHODOLOGY AND APPLICATION

The following WRF model parameters were chosen as potential predictors of the lightning occurrence: most unstable Convective Available Potential Energy (CAPE), K-Index (KI) (George, 1960), Total Totals Index (ITT) (Miller, 1967), 700-500 hPa lapse rate of equivalent potential temperature (θ_e) (Bolton, 1980), vertical velocity averaged between 850 hPa and 700 hPa (w), and ice mixing ratio integrated from 700 hPa to 500 hPa (QICE). According to the maximum and minimum values obtained from both WRF domains of 2 km grid resolution (DOM3$_{(0.5\text{-deg})}$ and DOM4$_{(1\text{-deg})}$), the parameters were divided into five evenly distributed ranges, as shown in Table 4, except the last. Due to the small values observed for the integrated ice mixing ratio, a different approach was considered for this variable in the development of the forecasting methodology to be discussed below.

The values of model variables computed at grid points close to lightning events detected by the BrasilDAT were compared to the corresponding values at all grid points. The hourly WRF outputs were compared to the coordinates of all flashes that occurred during the thunderstorm period. This analysis was made with 114960 CG flashes. The lightning data were used to classify the grid points, i.e., if there was at least one lightning within a square area of 1024 km^2 (radius = 16 km, diameter = 32 km) centered in each grid point of the WRF domain, the grid point was considered; otherwise, discarded. This area was defined based on the fact that the horizontal development of the stepped leader may precede its contact point on ground in 20 km or more (Krehbiel et al., 2000; Lang et al., 2004). The

values of model variables on the grid did not vary appreciably over the course of each thunderstorm period. This means that, if one lightning occurred only once close to a grid point, this grid point was taken into account for the whole period of the parent thunderstorm.

Figure 2 shows the ratios computed between the WRF grid points associated with lightning and all WRF grid points of $DOM3_{(0.5-deg)}$ and $DOM4_{(1-deg)}$. It is noticeable that the ratios increase monotonically as CAPE, KI, and ITT increases in magnitude. Similar behavior is observed for the average vertical velocity, except by the higher ratios for negative values in the first interval of the distributions, which may be related to the downdraft in the mature phase of thunderclouds. Regarding to the lapse rate of θ_e, the ratios increase smoothly with the instability degree. When the propitious conditions in the atmosphere are satisfied to have high values of the tested model variables, the potential to occur thunderstorms is also higher and, by consequence, the lightning incidence. Almost no differences are observed in the results of the ratios when the WRF simulations are performed with different resolutions of the GFS data.

Indices from 1 to 5 were assigned for the ratios to classify the variable ranges with an increasing probability of lightning occurrence. Table 5 shows how the index assignment was established. In general, the index 1 corresponds to the ratio of the first range; the index 2, to the ratio of the second range, and so on, until the fifth and last range which is assigned the index 5. In the case of the average vertical velocity, the index 5 is exceptionally assigned to the first ratio because of the strong downdraft current represented by the large incidence of negative values in the first interval. The index computation for the integrated ice mixing ratio is not exhibited in Table 5. This variable assumed null values in most of the model domain; then, if the index 1 was assigned for the first range of the ratio distribution, the probability of lightning occurrence would always be underestimated. So, due to the discrete character of the integrated ice mixing ratio, whenever the variable is greater than zero, the index is set as 5; otherwise, it is discarded.

An average was calculated using the indices of all variables for each grid point of the highest resolution domains. These average indices represent a probability in percentage of the lightning occurrence, and are indicated in the lightning forecasting maps (Figures 3 and 5). A very low probability for lightning occurrence is set by < 10% (~ index 1) and a very high chance for lightning is represented by > 90% (~ index 5).

To test the method for each case of WRF initialization, two other events were selected: one thunderstorm day, and one non-lightning day, as shown in Table 6. Figures 3 and 5 show the lightning forecasting results for (a) WRF runs with 1-degree GFS data, and (b) WRF runs with 0.5-degree GFS data. Figures 4 and 6 present GOES infrared satellite images. The analysis was only focused and performed during the maximum lightning occurrence instances. The black dots indicate the location of each flash detected by BrasilDAT.

Table 4 – Values intervals for the WRF meteorological variables of $DOM3_{(0.5-deg)}$ and $DOM4_{(1-deg)}$.

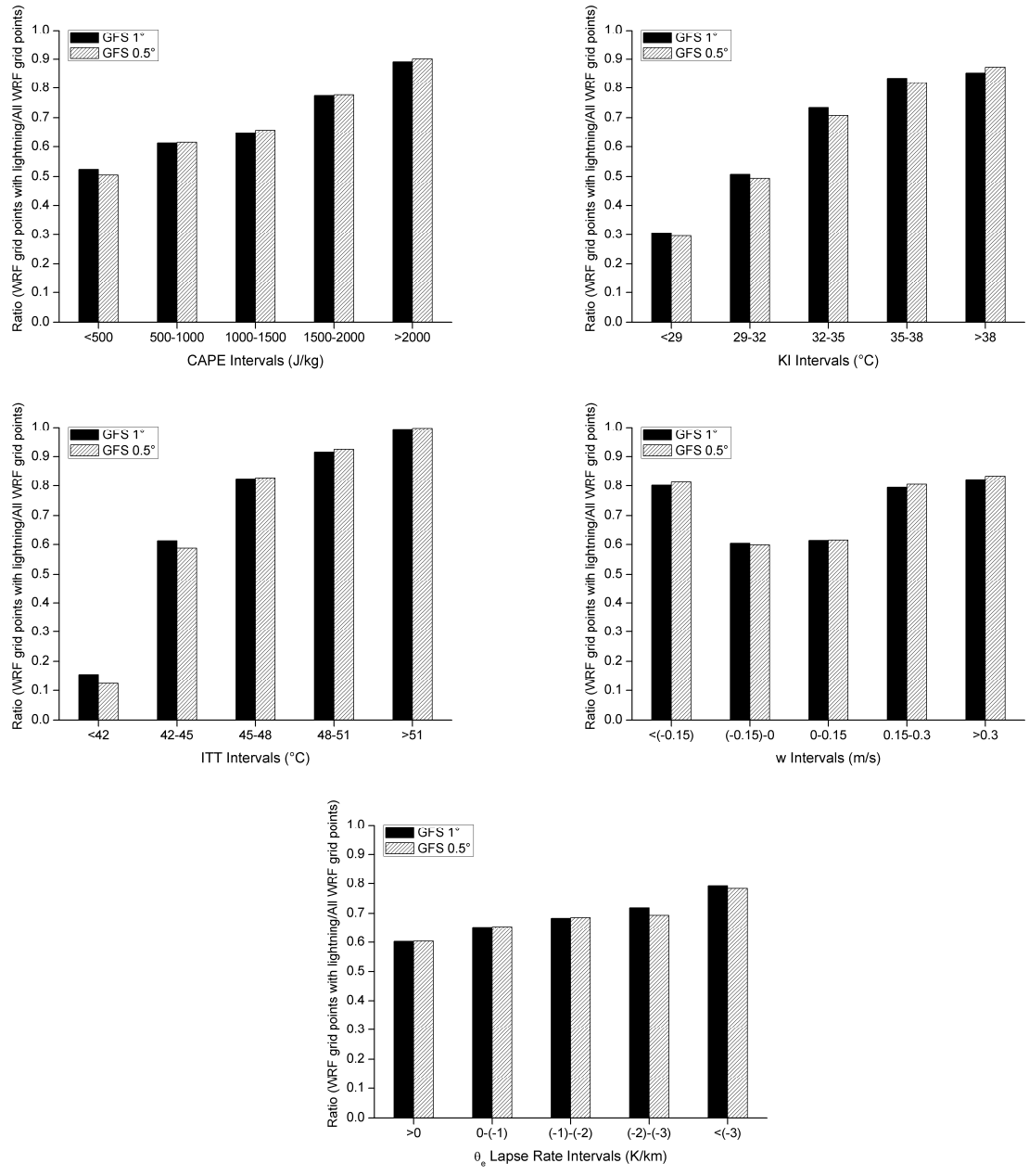| Variable	Values Intervals				
	1	2	3	4	5
CAPE (J/kg)	< 500	500 – 1000	1000 – 1500	1500 – 2000	> 2000
KI (°C)	< 29	29 – 32	32 – 35	35 – 38	> 38
ITT (°C)	< 42	42 – 45	45 – 48	48 – 51	> 51
Lapse Rate of θ_e (K/km)	> 0	0 – (-1)	(-1) – (-2)	(-2) – (-3)	< (-3)
w (m/s)	< (-0.15)	(-0.15) – 0	0 – 0.15	0.15 – 0.3	> 0.3

Figure 2 – Ratios between WRF grid points with lightning associated and all WRF grid points of DOM3$_{(0.5\text{-}deg)}$ and DOM4$_{(1\text{-}deg)}$, for CAPE, KI, ITT, 700-500 hPa lapse rate of θ_e, and average vertical velocity (w) between 850 and 700 hPa. The caption in the black rectangle shows both WRF initialization datasets under comparison.

Table 5 – Index assignment for the forecasting method.

Variable	Intervals	Ratios		Indices
		1-degree GFS	*0.5-degree GFS*	
CAPE (J/kg)	< 500	0.52	0.50	1
	500 – 1000	0.61	0.61	2
	1000 – 1500	0.65	0.66	3
	1500 – 2000	0.77	0.78	4
	> 2000	0.89	0.90	5
KI (°C)	< 29	0.30	0.29	1
	29 – 32	0.51	0.49	2
	32 – 35	0.73	0.71	3
	35 – 38	0.83	0.82	4
	> 38	0.85	0.87	5
ITT (°C)	< 42	0.15	0.12	1
	42 – 45	0.61	0.59	2
	45 – 48	0.82	0.83	3
	48 – 51	0.91	0.92	4
	> 51	0.99	1.00	5
Lapse rate of θ_e (K/km)	> 0	0.60	0.60	1
	0 – (-1)	0.65	0.65	2
	(-1) – (-2)	0.68	0.68	3
	(-2) – (-3)	0.71	0.69	4
	< (-3)	0.79	0.78	5
w (m/s)	< (-0.15)	0.80	0.81	5
	(-0.15) – 0	0.60	0.60	1
	0 – 0.15	0.61	0.61	2
	0.15 – 0.3	0.79	0.80	4
	> 0.3	0.82	0.83	5

*No index computation is showed for the integrated ice mixing ratio due to the large incidence of null values in model domains. So, if the variable is greater than zero, the index is set as 5; otherwise, it is discarded.

Table 6 – List of thunderstorm days used to test the forecasting method.

Date	Time Period	Total Flashes	Meteorological Condition
12/30/2008	1730-2230 UT	7041	Local convection due to a frontal system over the Atlantic Ocean
12/04/2008	1530-2230 UT[a]	0	Partly Cloudy (Low Cloudiness)
Total:	**12 hours**	**7041 flashes**	

[a]Similar time period of the thunderstorm analysis.

A chance greater than 50% was assigned for lightning occurrence in the upper side of Figures 3a and 3b, where is observed a flash concentration. Over the remaining area, no flash was detected, and smaller probabilities were forecasted for the lightning activity. There are no differences between Figures 3a and 3b, which may indicates that the resolution of GFS input data does not affect significantly the lightning prediction. The convective activity evident in the GOES infrared satellite image (Figure 4) over northern São Paulo state and southern Minas Gerais was spatially well characterized by the forecasting methodology.

Figure 5 presents the application of the forecasting method for a day without lightning occurrence. The probabilities are lower than 50% in both maps for the entire domain, and could be associated with the stratiform clouds observed in the GOES infrared satellite image (Figure 6) over the Minas Gerais and São Paulo states. Again no differences are verified comparing both maps.
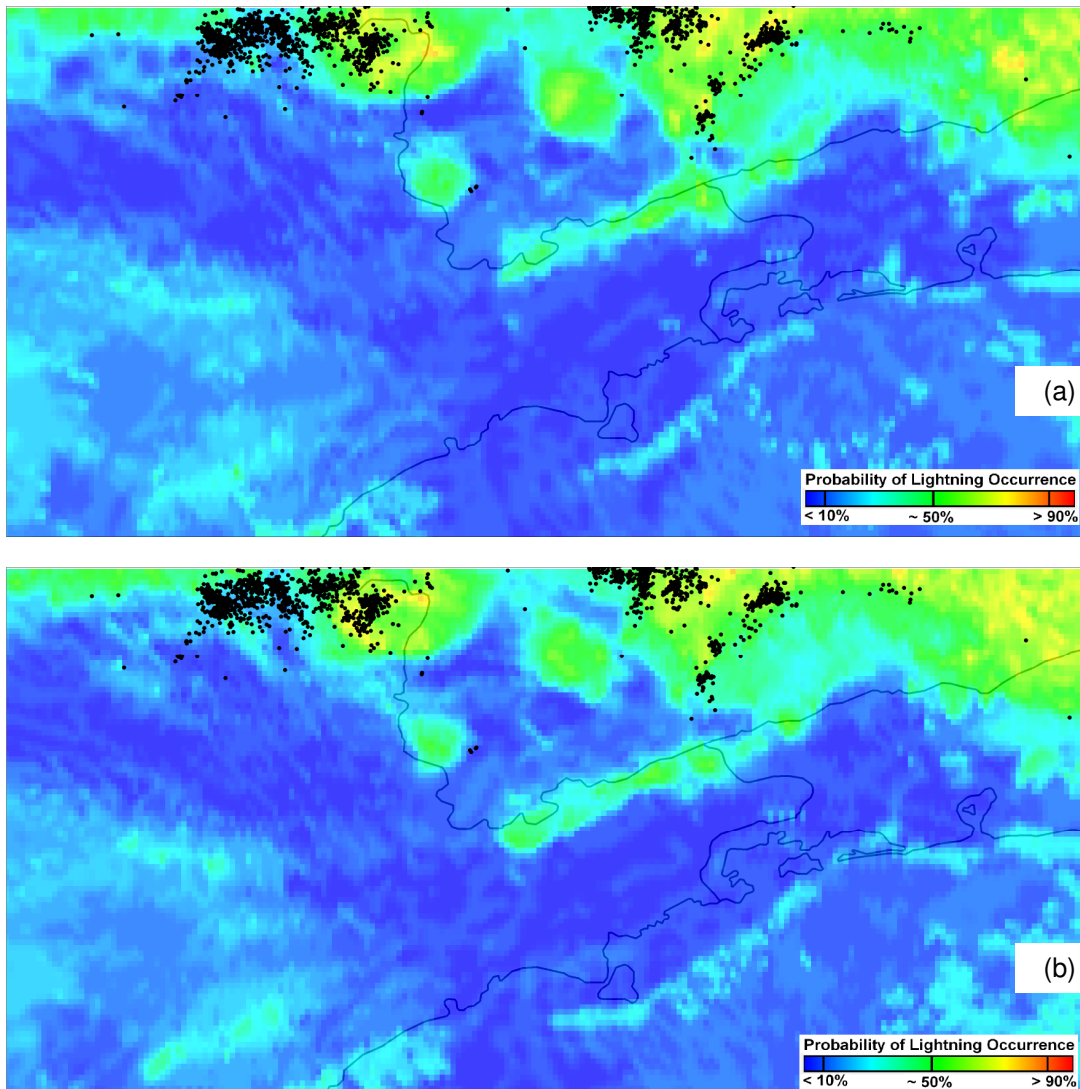

Figure 3 – Lightning forecasting maps for December 30, 2008 at 19 UT. (a) WRF runs with 1-degree GFS input data, and (b) WRF runs with 0.5-degree GFS input data. The black dots indicate the location of 1911 flashes detected by BrasilDAT from 1830 UT to 1930 UT.
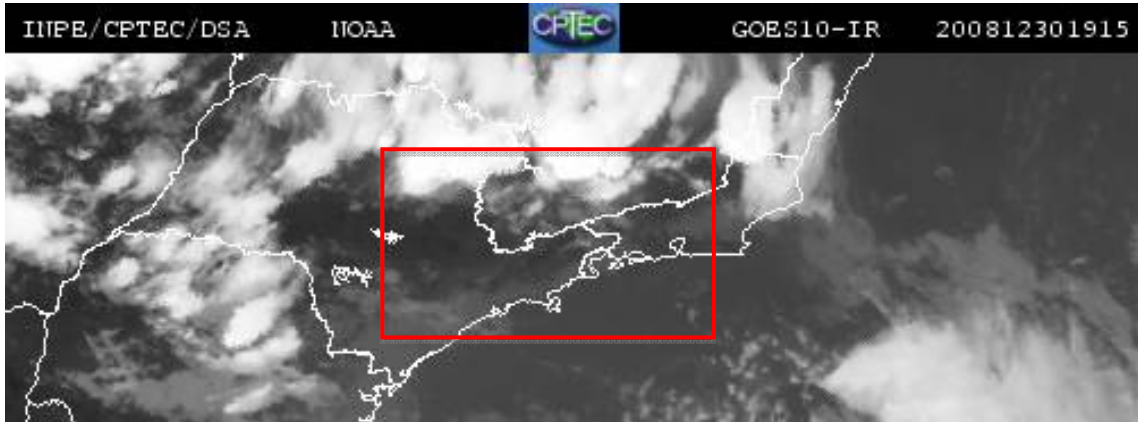
Figure 4 – GOES-10 infrared satellite image for December 30, 2008 at 1915 UT. The red rectangle indicates the location of the region of interest.
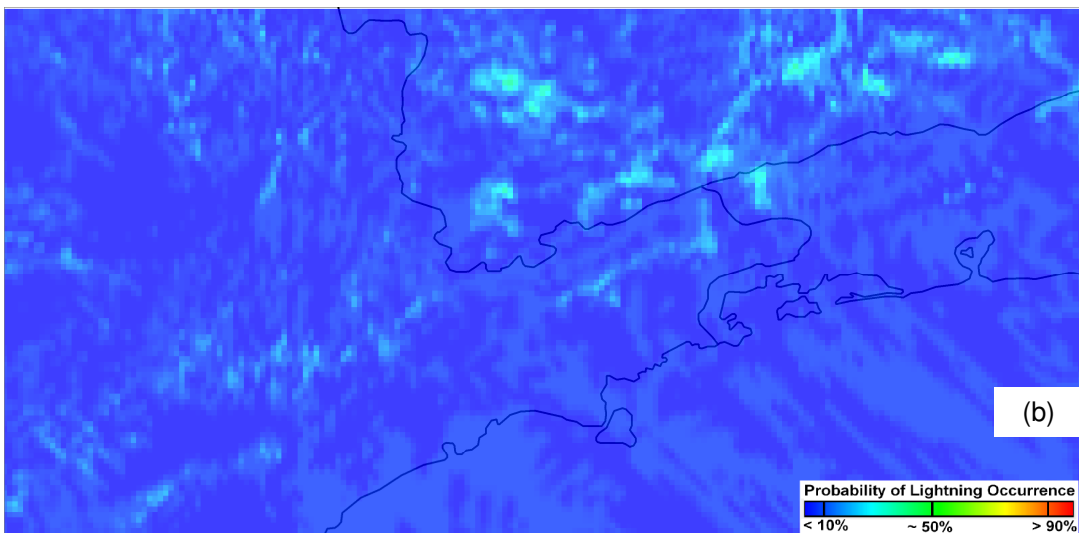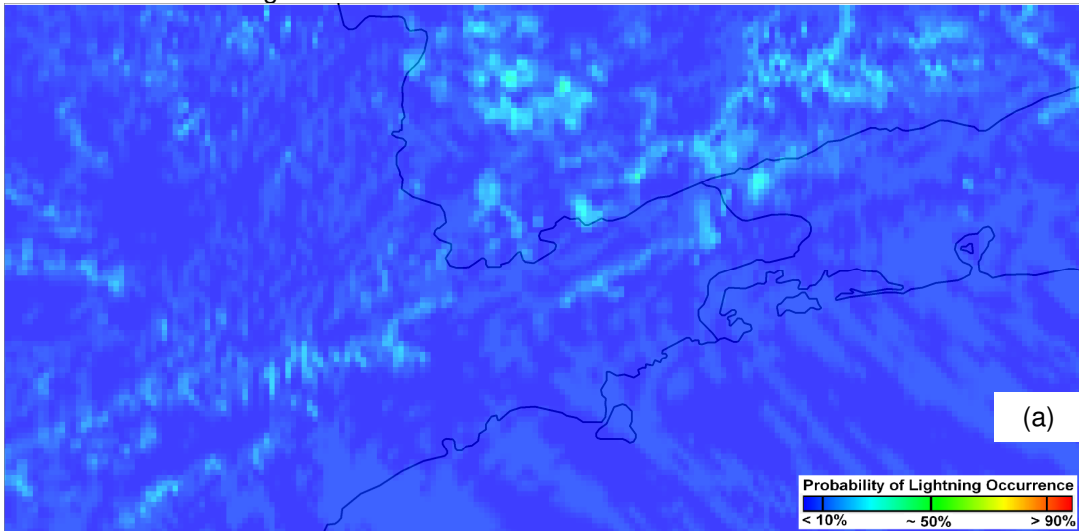

Figure 5 – Lightning forecasting maps for December 04, 2008 at 19 UT. (a) WRF runs with 1-degree GFS input data, and (b) WRF runs with 0.5-degree GFS input data. No flash was detected by BrasilDAT.
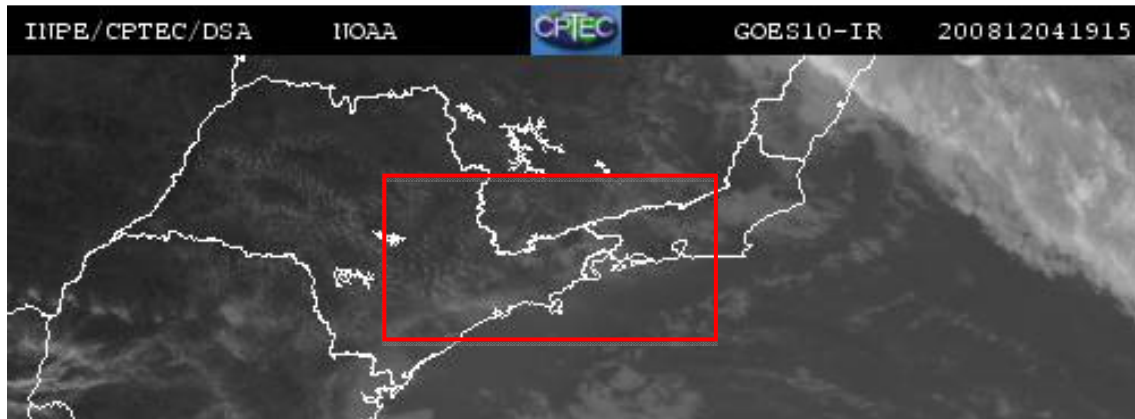
Figure 6 – GOES-10 infrared satellite image for December 04, 2008 at 1915 UT. The red rectangle indicates the location of the region of interest.

5. STATISTICAL ANALYSES

A statistical evaluation of the lightning forecasting developed from WRF runs using different resolutions of GFS data was performed using the following scores: Probability of Detection – POD (equation 1), False Alarm Ratio – FAR (equation 2), Critical Success Index – CSI (equation 3), and Accuracy – ACUR (equation 4):

$$POD = (a) / (a+c) \qquad (1)$$
$$FAR = (b) / (a+b) \qquad (2)$$
$$CSI = (a) / (a+b+c) \qquad (3)$$
$$ACUR = (a+d) / (a+b+c+d) \qquad (4)$$

with "a", "b", "c", and "d" defined in Table 7. These quantities represent the sums of the WRF grid points that satisfied some combinations between the lightning occurrence or not, and a threshold chosen as 2.5 (the indices vary from 1 to 5) for the index value.

Figure 7 presents the skill scores for the eleven thunderstorm cases studied (see Table 1 and 6). The perfect scores are 1 for POD, CSI and ACUR, and 0 for FAR. POD showed that the skill for the lightning forecasting based on WRF runs with 0.5-degree GFS data is slightly better than those with 1-degree resolution. In average, more than 70% of the observed regions of lightning occurrence were correctly predicted. Except for a single case, the FAR values were nearly coincident for a same thunderstorm. Almost 20% of the forecasted regions of lightning occurrence were not observed. Considering all thunderstorms investigated, the CSI indicates

that more than half of the regions of lightning occurrence (observed and/or predicted) were correctly forecasted. The 0.5-degree GFS data guarantees slightly higher CSI values for the lightning forecasting comparing to the other data resolution, in agree with the POD results. The accuracy indicates that about 60-80% of all forecasted regions of lightning occurrence were correct. Again small differences were observed in the ACUR values for each thunderstorm, although the scores representing the 0.5-degree GFS data were slightly the highest ones.

6. CONCLUSION

The objective of this work was to evaluate the sensitivity of the lightning forecasting method using different resolutions of GFS input data to initialize the WRF model. Besides the comparison between the forecasting maps for two thunderstorm events, the statistical scores POD, FAR, CSI, and ACUR were computed to help in the evaluation.

The results showed that the resolution of the GFS data used to initialize the WRF model does not affect substantially the lightning forecasting. Some details in the WRF outputs, after the integration, seem to be too smoothed independent of the resolution of the input data. It seems that higher resolution input data is required to the model better characterize the meteorological information at very high resolutions (2 km and lower). The use of data assimilation and new types of observations resulting in better initial conditions for the atmospheric models may contribute to improve

the model products even without changing the resolution of the input data.

In future works the technique of data assimilation will be tested, and the benefits for lightning forecasting will be evaluated.

Table 7 – Combination of physical conditions required to define "a", "b", "c", and "d".

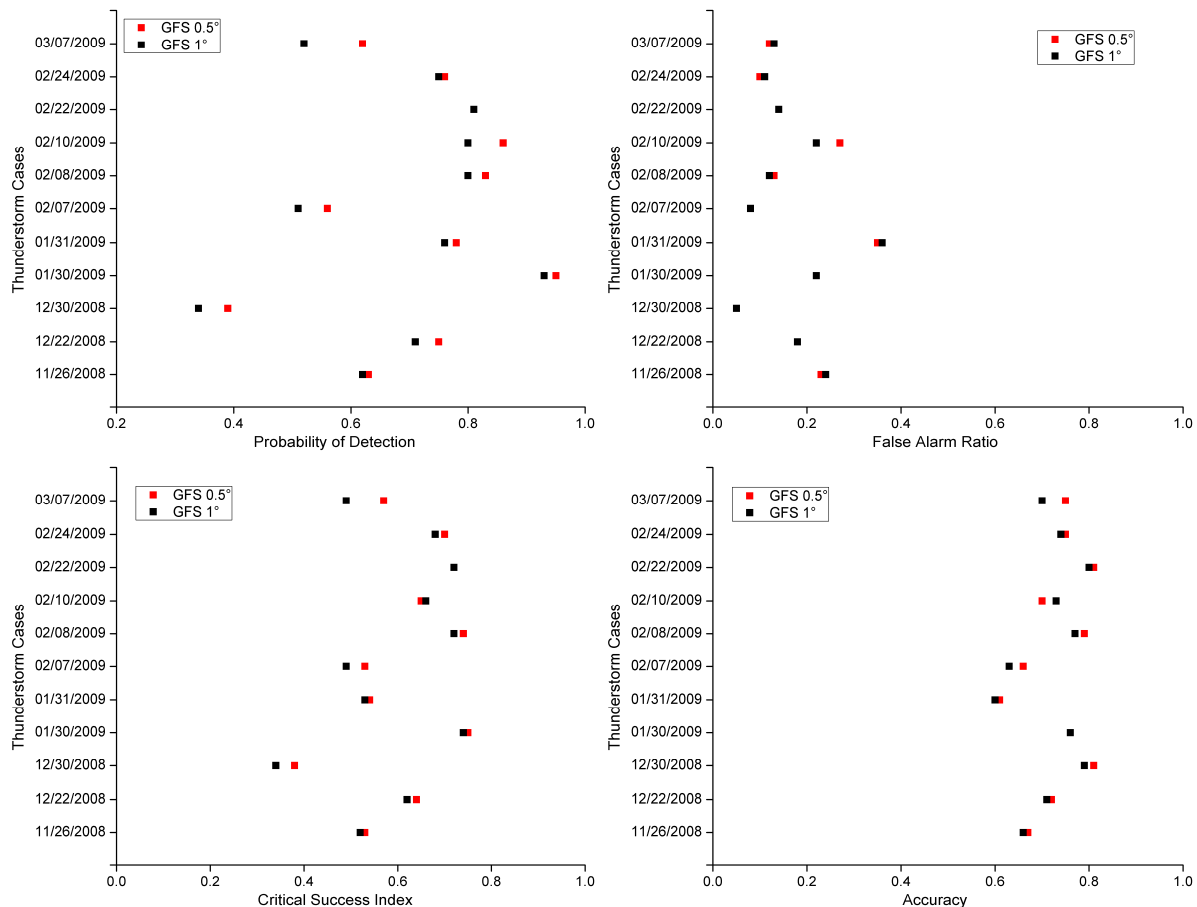| Variable	Is there lightning in the vicinity of grid point?	Does the value of the index grid point exceed a specific threshold?
a	yes	yes
b	no	yes
c	yes	no
d	no	no

Figure 7 – Statistical scores: Probability of Detection (POD), False Alarm Ratio (FAR), Critical Success Index (CSI), and Accuracy (ACUR), calculated based on the eleven thunderstorm cases.

7. REFERENCES

Ballarotti, M. G., Saba, M. M. F., Pinto Jr., O., 2006: A new performance of evaluation of the Brazilian lightning location system (Rindat) based on high-speed camera observations of natural negative ground flashes. In: International Lightning Detection Conference, 19, 24-25 April 2006, Tucson. **Proceedings**…Tucson: [s.n].

Bolton, D., 1980: The computation of equivalent potential temperature. *Mon. Weather Rev.*, **108**(7), 1046-1053.

Chen, F., and Dudhia, J., 2001: Coupling an advanced land-surface/ hydrology model with the Penn State/ NCAR MM5 modeling system. Part I: Model description and implementation. *Mon. Weather Rev.*, **129**, 569-585.

Dudhia, J., 1989: Numerical study of convection observed during the winter monsoon experiment using a mesoscale two-dimensional model. *J. Atmos. Sci.*, **46**, 3077-3107.

George, J. J., 1960: *Weather forecasting for aeronautics*. New York: Academic Press. 673 p.

Grell, G. A., and Devenyi, D., 2002: A generalized approach to parameterizing convection combining ensemble and data assimilation techniques. *Geophys. Res. Lett.*, **29**(14), 1693.

Krehbiel, P. R., Thomas, R. J., Rison, W., Hamlin, T., Harlin, J., Davis, M., 2000: GPS-based mapping system reveals lightning inside storms. *Eos, Trans. Amer. Geophys. Union*, **81**(3), 21.

Lang, T. J., Rutledge, S. A., Wiens, K. C., 2004: Origins of positive cloud-to-ground lightning flashes in the stratiform region of a mesoscale convective system. *Geophys. Res. Lett.*, **31**(L10105).

Lorenz, E. N., 1965: A study of the predictability of a 28-Variable Atmospheric Model. *Tellus*, **17**(3), 321-333.

Miller, R. C., 1967: Note on analysis and severe storm forecasting procedures of the Military Weather Warning Center. *AWS Tech. Rep. 200*, USAF, Scott AFB, IL, 94 pp.

Mlawer, E. J., Taubman, S. J., Brown, P. D., Iacono, M. J., Clough, S. A., 1997: Radiative transfer for inhomogeneous atmosphere: RRTM, a validated correlated-k model for the longwave. *J. Geophys. Res.*, **102**(D14), 16663-16682.

Noh, Y., Cheon, W. G., Hong, S-Y., Raasch, S., 2003: Improvement of the K-profile model for the planetary boundary layer based on large eddy simulation data. *Bound.-Layer Meteor.*, **107**, 401–427.

Pinto Jr., O., 2009: *Lightning in the tropics: from a source of fire to a monitoring system of climate changes*. Nova Science Publishers, 109 p.

Pinto Jr., O., Pinto, I. R. C. A., Naccarato, K.P., 2007: Maximum cloud-to-ground lightning flash densities observed by lightning location systems in the tropical region: A review. *Atmos. Res.*, **84**, 189-200.

Saraiva, A. C. V., Saba, M. M. F., Pinto Jr., O., Cummins, K. L., Krider, E. P., 2011: Analyses of the key factors that may lead to a misclassification of negative flashes reported by lightning locating systems (LLS). *Atmos. Res.* (submitted).

Skamarock, W. C.; Klemp, J. B.; Dudhia, J.; Gill, D. O.; Barker, D. M.; Duda, M. G., Huang, X-Y, Wang, W.; Powers, J. G., 2008: A description of the Advanced Research WRF Version 3. *NCAR Tech. Notes*.

Thompson, G., Rasmussen, R. M., Manning, K., 2004: Explicit forecasts of winter precipitation using an improved bulk microphysics scheme. Part I: Description and sensitivity analysis. *Mon. Weather Rev.*, **132**, 519-542.

Warner, T. T., Peterson, R. A., Treadon, R. E., 1997: A tutorial on lateral boundary conditions as a basic and potentially serious limitation to regional weather prediction. *Bull. Amer. Meteor. Soc.*, **78**, 2599-2617.